Supplementary Information

On the dehydrogenation mechanism during incubation period in nanocrystalline MgH₂

Apurva Shantilal Gangrade, Akhil Aditya Varma, Nikhil Kishor Gor, Sweta Shriniwasan,

Sankara Sarma V. Tatiparti*

Department of Energy Science & Engineering, Indian Institute of Technology

Bombay, Mumbai-400076, India

*Corresponding author Email: sankara@iitb.ac.in

S1. Refinement parameters obtained from XRD patterns

Table S1 (A) Atomic parameters of MgH_2 refined from the XRD patterns of the powders dehydrogenated at 320 and 350 °C

| Temperature (°C)	Time	Positional parameters			B ($Å^2$)	
		H (4*f*)			Mg	H
320 °C	0	0.30787(303)	0.30787(303)	0	0.146(56)	1.292(774)
	35	0.32391(343)	0.32391(343)	0	1.122(0)	1.382(0)
	60	0.31172(248)	0.31172(248)	0	0.704(0)	0.363(0)
350 °C	0	0.31173(208)	0.31173(208)	0	0.672(0)	0.85(0)
	5	0.32419(717)	0.32419(717)	0	1.988(0)	0.25(0)
	11	0.31720(536)	0.31720(536)	0	0.02(43)	1.293(873)

Table S1 (B) Unit cell parameters of MgH_2 refined from the XRD patterns of the powders dehydrogenated at 320 and 350 °C

Temperature (°C)	Time (min)	*a* (Å)	*c* (Å)	*c/a*	Unit cell Volume ($Å^3$)
320	0	4.5187(1.2)	3.0218(1.4)	0.6687(.270)	61.7008(674)
	35	4.5141(1.5)	3.0185(1.8)	0.6687(.100)	61.5095(430)
	60	4.5148(1.1)	3.0192(1.3)	0.6687(.097)	61.5417(244)
350	0	4.5186(0.8)	3.0221(.9)	0.6688(.038)	61.7040(186)
	5	4.5165(3.4)	3.0207(3.4)	0.6688(.038)	61.6171(315)
	11	4.5183(1.2)	3.0220(1.4)	0.6688(.076)	61.6940(128)

Table S1 (C) Agreement parameters of MgH$_2$ refined from the XRD patterns of the powders dehydrogenated at 320 and 350 °C

Temperature (°C)	Time	R_p	R_{wp}	R_{exp}	χ^2
320 °C	0	4.61	7.95	2.60	9.35
	35	6.47	9.73	3.52	7.63
	60	4.95	7.08	3.53	4.03
350 °C	0	4.20	6.13	2.57	5.70
	5	6.92	10.9	3.59	9.17
	11	6.48	10.6	4.05	6.80

where R_p is profile factor R_{wp} is weighted profile factor, R_{exp} is expected weighted profile factor and χ^2 goodness of fit indicator.
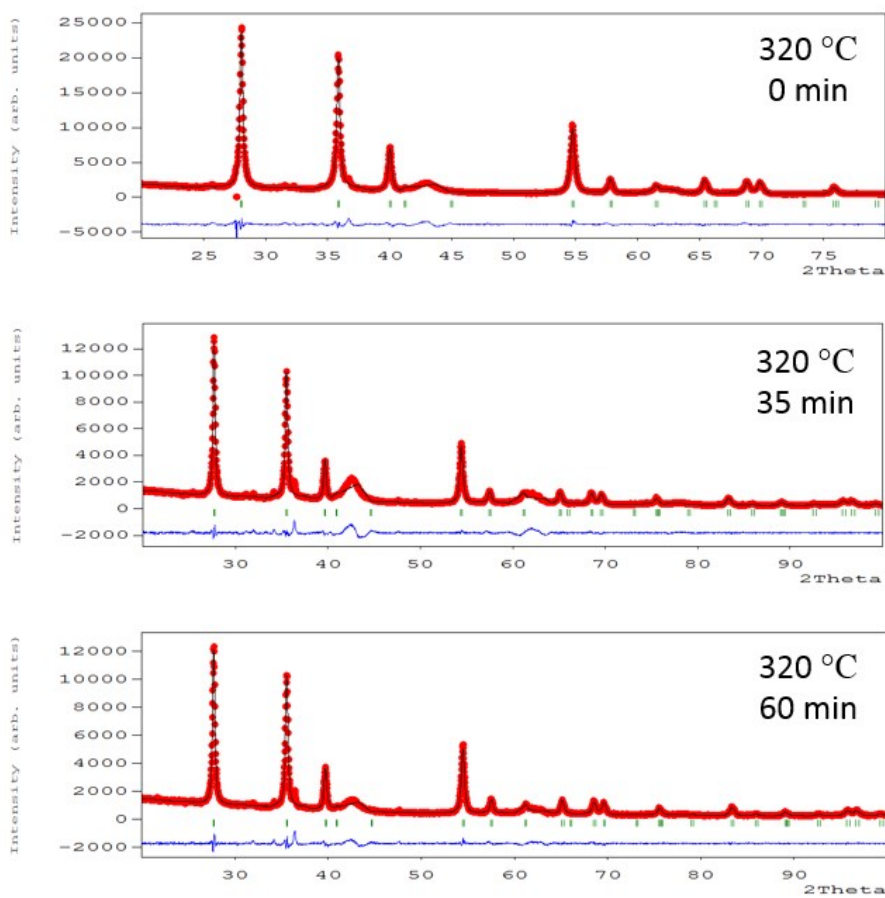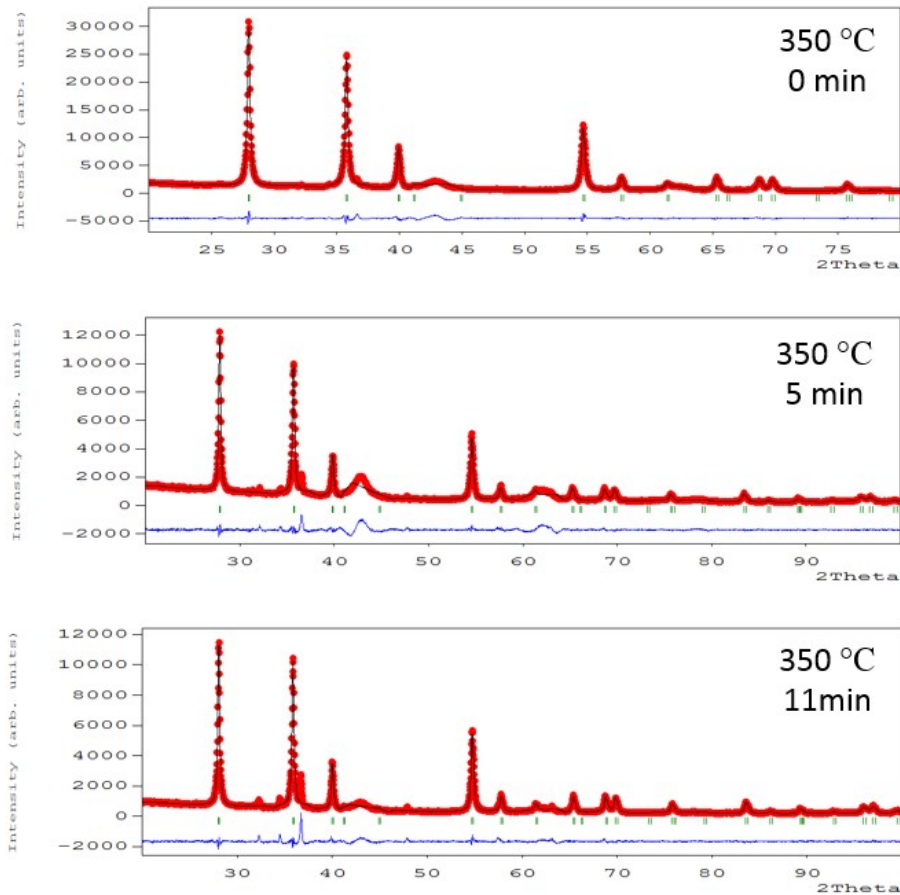
Fig. S1 Refined XRD curves of powders dehydrogenated at 320 and 350 °C.

S2. Volume fraction analysis of phases observed in TEM diffraction patterns

The following steps are implemented to estimate the fraction of Mg formed at different regimes of the Dark Field images:

1. Particle in the TEM was divided into smaller contours by normalizing the distance of surface from the centroid.

2. Area of Mg in the respective contours, total area of all the contours, aspect ratio and centroid was calculated by using ImageJ software (Version 1.48).

3. Area to volume conversion has been done by the stereographic conversion from 2D to 3D as described by Sahagian and Proussevitech[1]. This conversion was done using the area fraction (N_{Ai}) of each particle and its corresponding aspect ratio using

ImageJ software. Using the average aspect ratio, the area fraction (N_{Ai}) was converted to the corresponding volume fraction (N_{Vi}) using the literature conversion factor in terms of probabilities ($P_{i,j+1}$) and using the Eq.1[1].

$$N_{Vi} = \frac{1}{P_{i,1}H'_i}\left(N_{Ai} - \sum_{j=1}^{i-1} P_{i,j+1}H'_{i+1}N_{Vi(i-j)} \right) \tag{1}$$

where,

$P_{i,j+1}$ = intersection probabilities of particle geometry (obtained from literature based on aspect ratio and class size)

H'_i = mean projected height corresponding to the area. $P_{i,j+1}$.

Using Eq.1, volume fraction distribution of dehydrogenated MgH_2 powders is obtained.

Based on these calculations the volume fractions are represented as follows
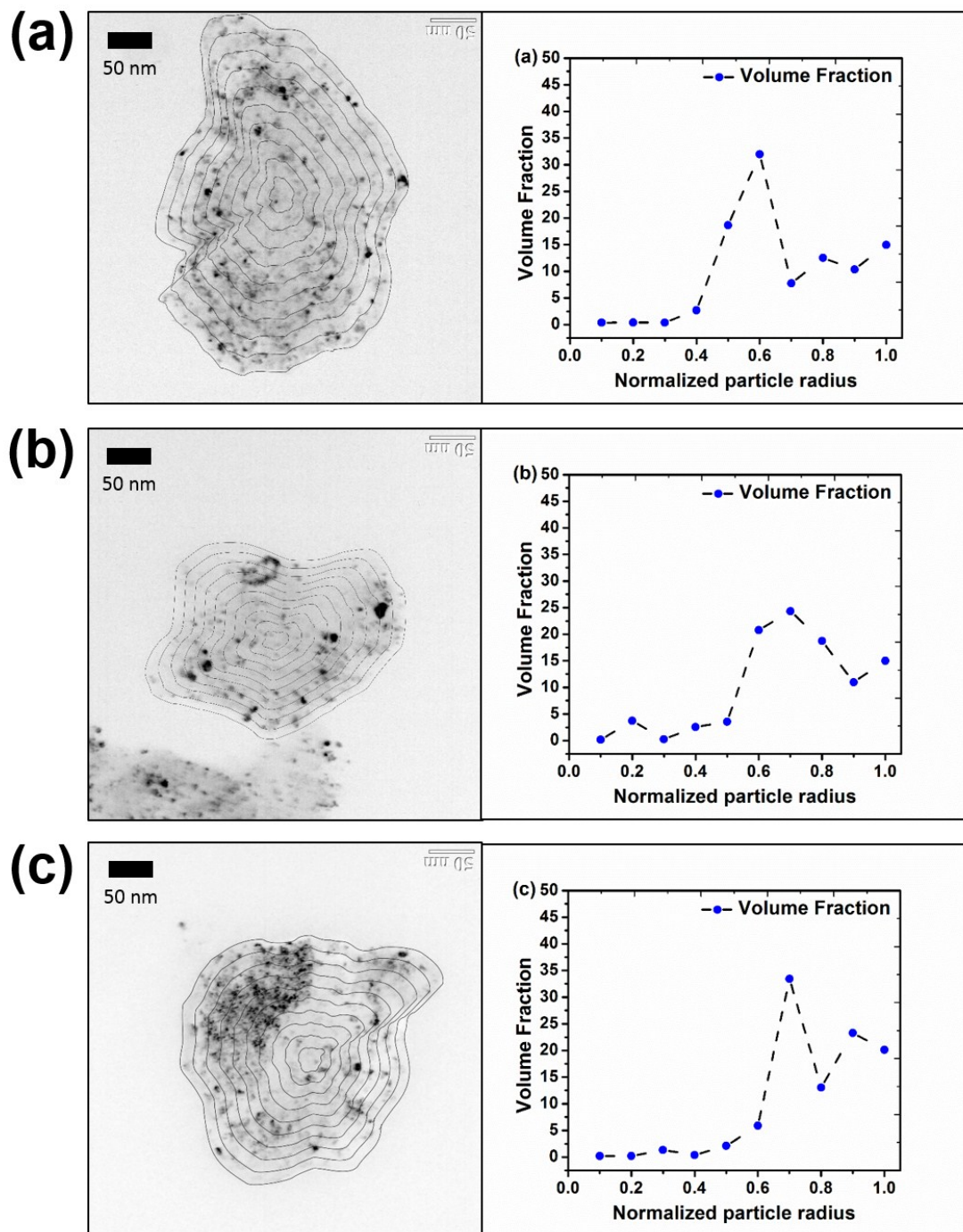
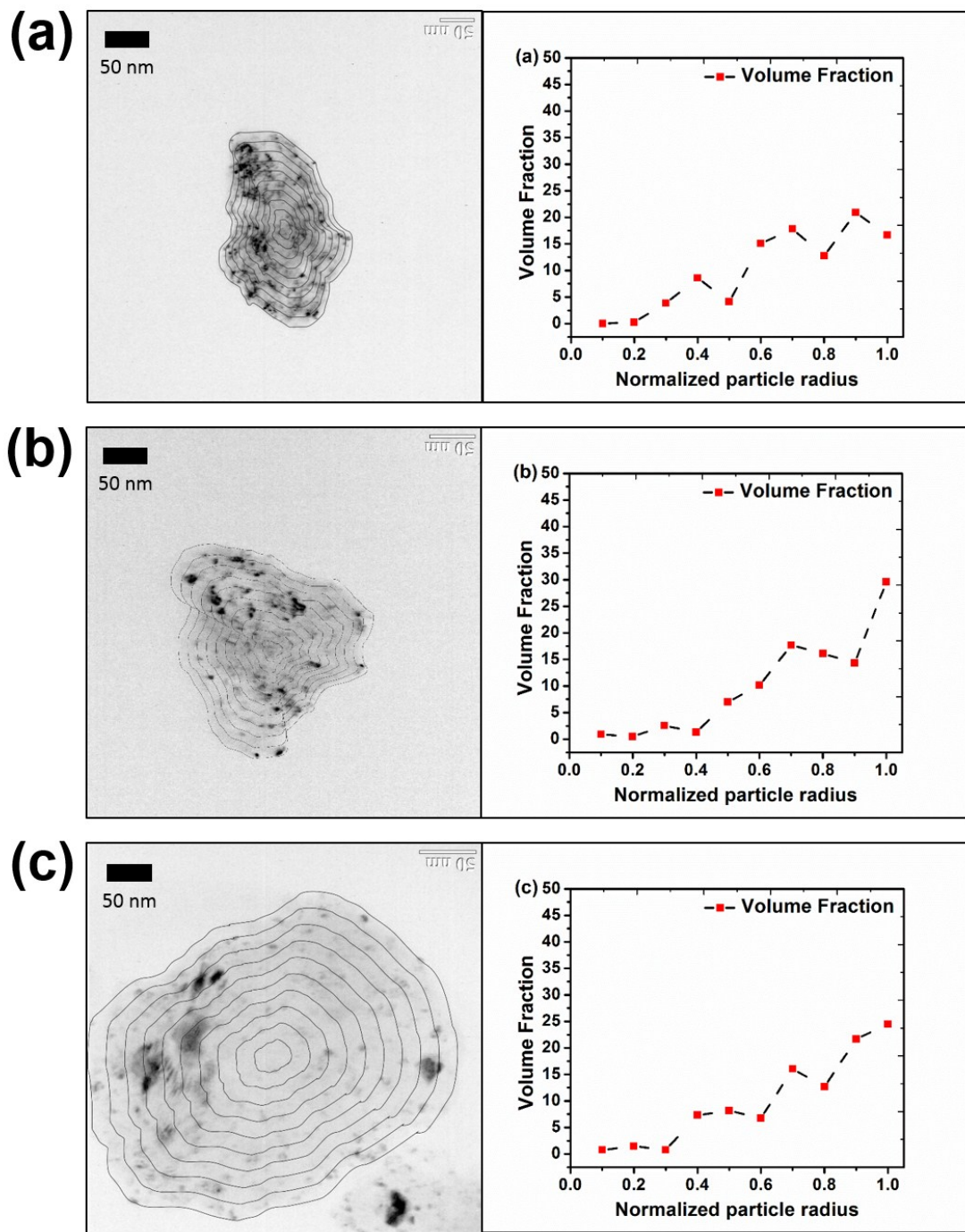Fig. S2 (A) Volume fraction analysis of Mg phase in powders dehydrogenated at 320 °C.

Fig. S2 (B) Volume fraction analysis of Mg phase in powders dehydrogenated at 350 °C.

S3. Charge density distribution maps

The charge density maps were obtained from Fourier transforms of the observed structure factors using maximum entropy method (MEM) using Fullprof Suite program. The *F*-constraint to the MEM scattering data is given by Eq.2[2]

$$C_F = \chi_{aim}^{2} + \frac{1}{N_F}\left(\frac{\left|F_{obs}(H_i) - F_{MEM}(H_i)\right|}{\sigma(H_i)}\right)^{2} = 0 \qquad (2)$$

where, H_i is the scattering vector of Bragg reflection, $F_{obs}(H_i)$ is the observed structural factor of H_i, $F_{MEM}(H_i)$ is the structure factor for MEM, N_F is the number of reflections, $\sigma(H_i)$ is the standard deviation in H_i, for convergence criterion χ_{aim}^{2} is set to 1. The Fourier transform of $F_{MEM}(H_i)$ gives the respective charge density distribution maps[2].
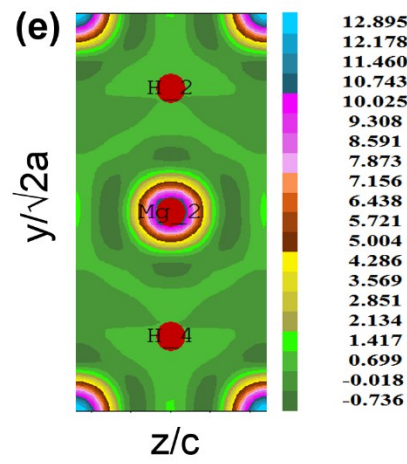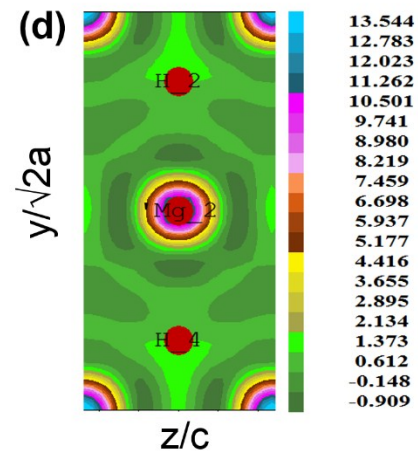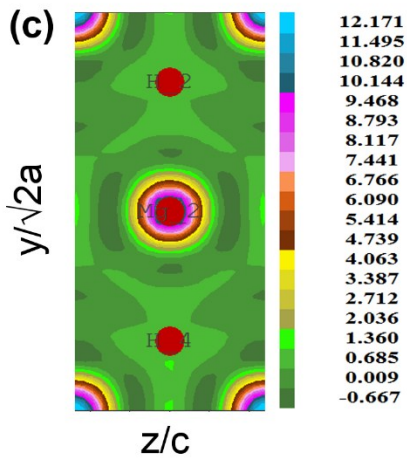
320 °C

(a)

(b)

350 °C

(c)

(d)

(e)

(f)
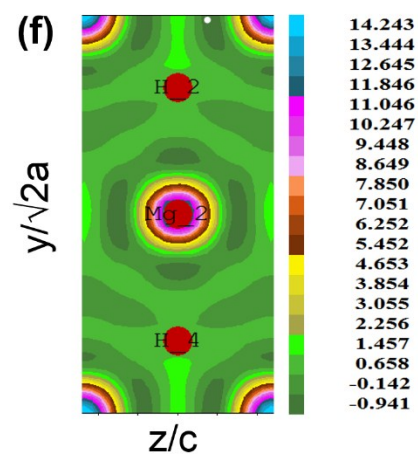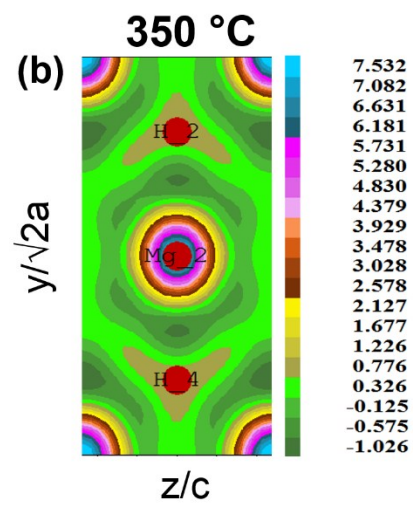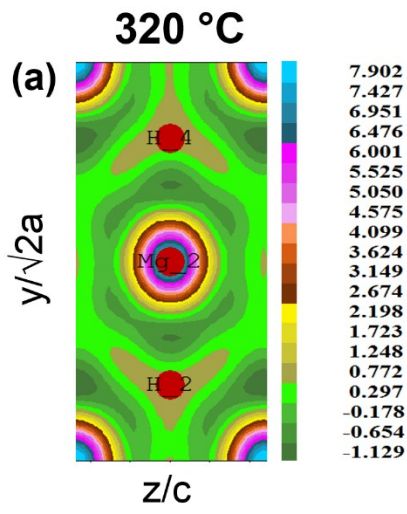
Fig. S3 Charge density maps of MgH$_2$ in {11$\bar{2}$0} plane in powders dehyrogenated at 320 and 350 °C.

S4. The growth dimensionality (*n*) values with standard uncertainties"(error bars indicate ±σ)".
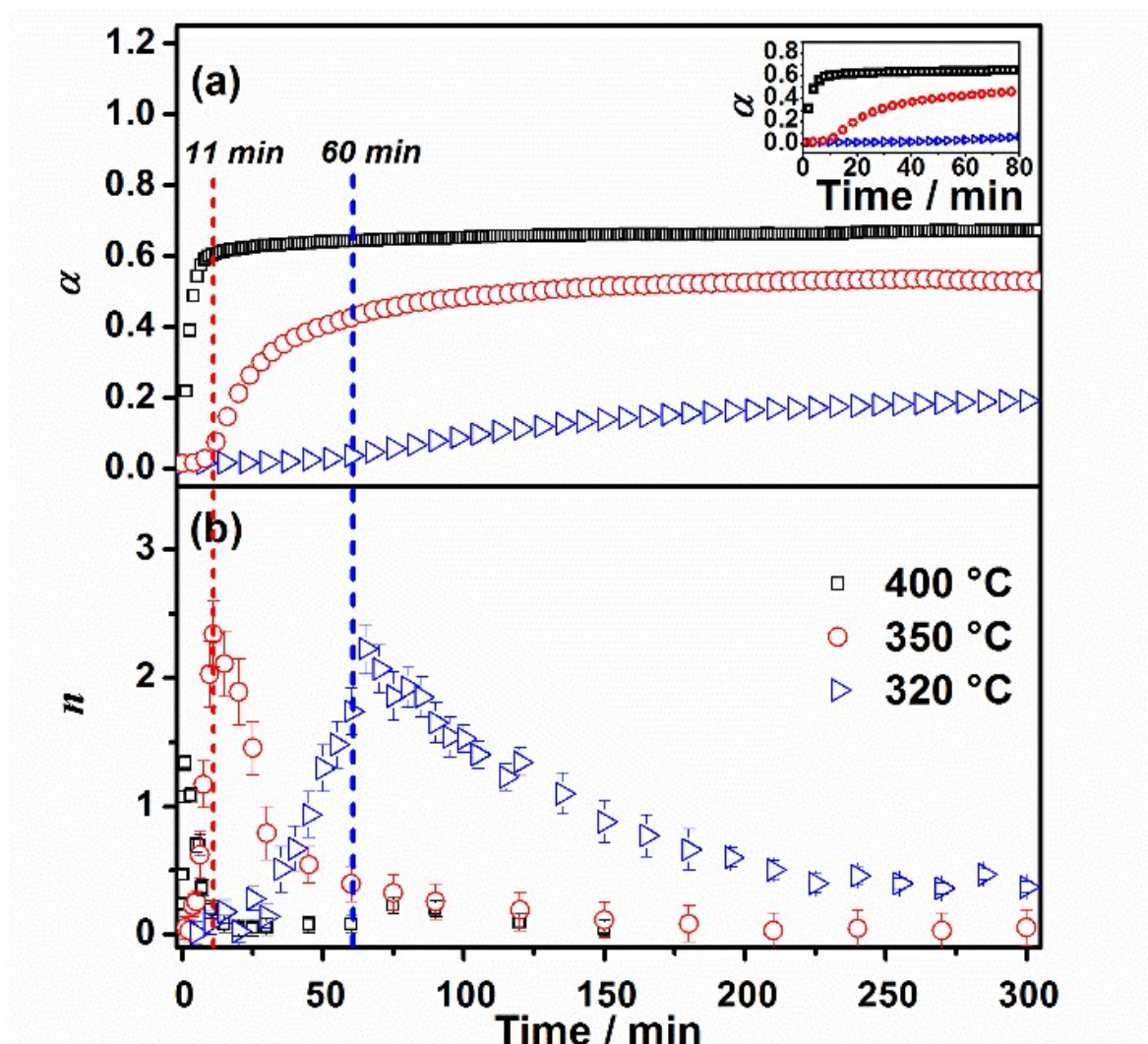

Fig. S4 *n* values with standard uncertainties.

S5. Estimation of activation energies for nucleation and growth during incubation period.

For estimation of activation energies dehydrogenation data at four different temperatures namely 320, 335, 350 and 400 °C are considered. The corresponding α-t and n-t curves are shown in Figs. S5 (A) and S5 (B), respectively.
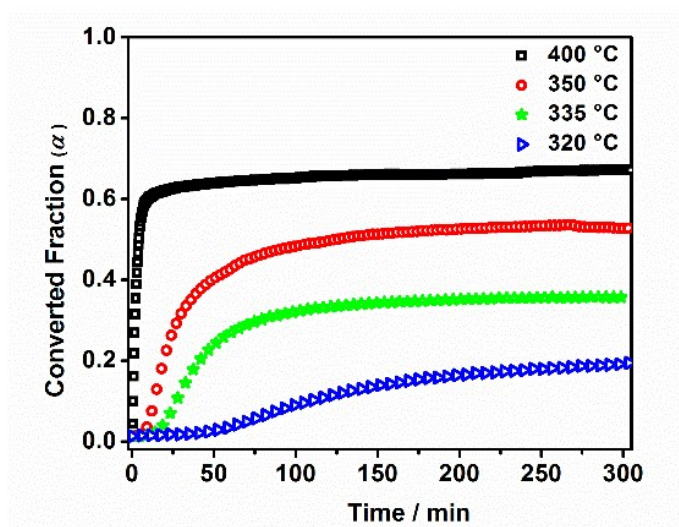

Fig. S5 (A) Converted fraction-time (α-t) of MgH$_2$ to Mg with dehydrogenation time for 320, 335, 350, and 400 °C.
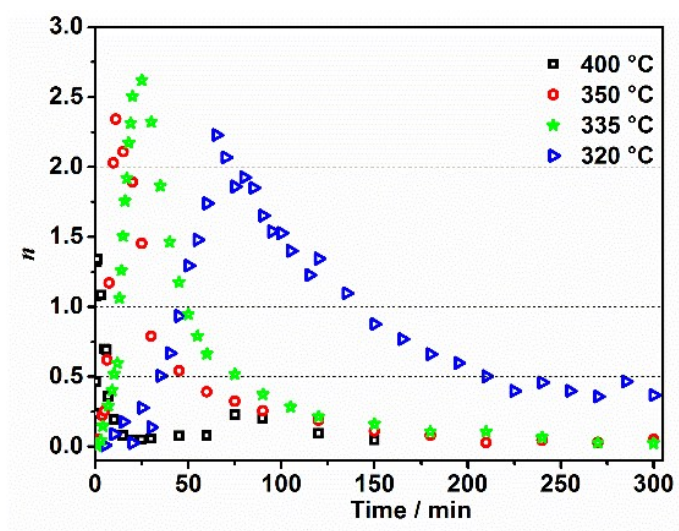

Fig. S5 (B) Growth dimensionality (n) with dehydrogenation time for 320, 335, 350, and 400 °C.

The kinetic factor k for the reaction between Mg and MgH_2 is given as

$$k = k_g N_o U^n$$

where k_g: geometric factor ($=4\pi/3$: sphere ; $=8$: cube), N_o: number of available nucleation sites per unit volume of the particle and U: Mg/MgH_2 interface velocity[3].

Table S5. Estimated $k_g N_o$ and U from $\ln(k)$ versus n plot during incubation period.

Temperature (°C)	U	$k_g N_o$
320	0.000351	0.020038
335	0.001283	0.018867
350	0.005775	0.035300
400	0.065100	0.027100

The estimated activation energies for nucleation (from $k_g N_o$) and growth (from U) are 12±2 and 209±8 kJ/mol H, respectively.
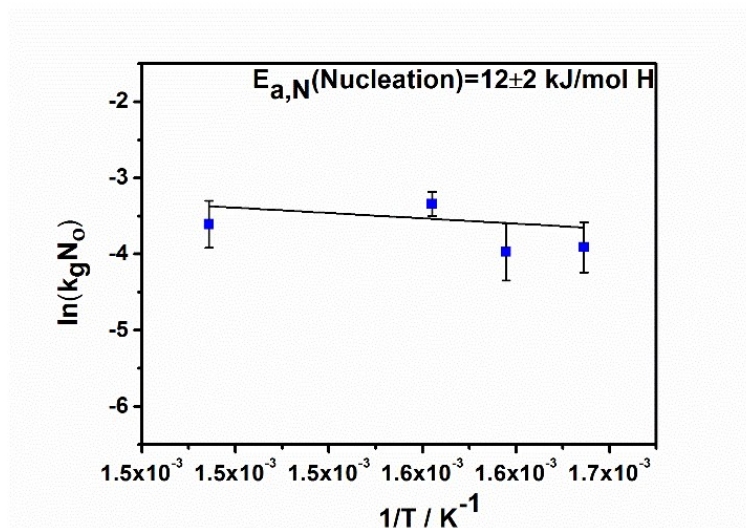

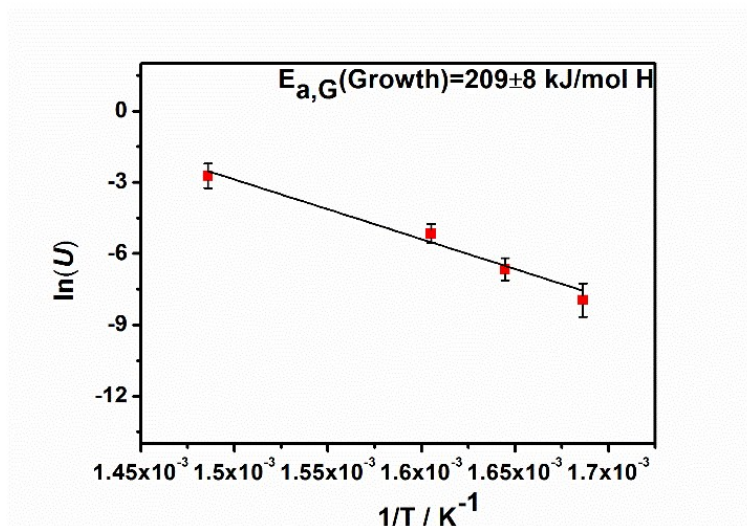Fig. S5 (C) $\ln(k_g N_o)$-$1/T$ plot for estimation of activation energy for Nucleation (error bars indicate ±σ).

Fig. S5 (D) ln(U)-1/T plot for estimation of activation energy for Growth (error bars indicate ±σ).

References

1. D. L. Sahagian and A. A. Proussevitch, *J. Volcanol. Geoth. Res.*, 1998, **84**, 173-196.

2. N. Bindzus and B. B. Iversen, *Acta Crystallogr. Sect. A*, 2012, **68**, 750-762.

3. M. H. Mintz and Y. Zeiri, *J. Alloys Compd.*, 1995, **216**, 159-175.